Ultrasmooth Gold Thin Films by Self-Limiting Galvanic Displacement on Silicon

ARTICLE *in* ACS APPLIED MATERIALS & INTERFACES · MAY 2011

Impact Factor: 6.72 · DOI: 10.1021/am200144k · Source: PubMed

3 AUTHORS:

Albert Gutés
University of California, Berkeley
27 PUBLICATIONS **767** CITATIONS
SEE PROFILE

C. Carraro
University of California, Berkeley
193 PUBLICATIONS **4,665** CITATIONS
SEE PROFILE

Roya Maboudian
University of California, Berkeley
236 PUBLICATIONS **7,054** CITATIONS
SEE PROFILE

ACS APPLIED MATERIALS & INTERFACES

RESEARCH ARTICLE

www.acsami.org

Ultrasmooth Gold Thin Films by Self-Limiting Galvanic Displacement on Silicon

Albert Gutés, Carlo Carraro, and Roya Maboudian*

Department of Chemical and Biomolecular Engineering, University of California at Berkeley, Berkeley, California, 94720, United States

ABSTRACT: Galvanic displacement (GD), a type of electroless deposition, has been used to obtain ultrasmooth gold thin films on silicon ⟨111⟩. The novel aspect of the method presented herein is the absence of fluoride ions in the liquid phase, and its principal advantage when compared to previous efforts is that the process is inherently self-limiting. The self-limiting factor is due to the fact that in the absence of fluorinated species, no silicon oxide is removed during the process. Thus, the maximum gold film thickness is achieved when elemental silicon is no longer available once the surface is oxidized completely during the galvanic displacement process. X-ray photoelectron spectroscopy has been used as a tool for thickness measurement, using the gold to silicon ratio as an analytical signal. Three gold plating solutions with different concentrations of $KAuCl_4$ (2, 0.2, and 0.02 mM) have been used to obtain information about the formation rate of the gold film. This XPS analysis demonstrates the formation of gold films to a maximum thickness of ~3.5 Å. Atomic force microscopy is used to confirm surface smoothness, suggesting that the monolayer growth does not follow the Volmer−Weber growth mode, in contrast to the GD process from aqueous conditions with fluorinated species.

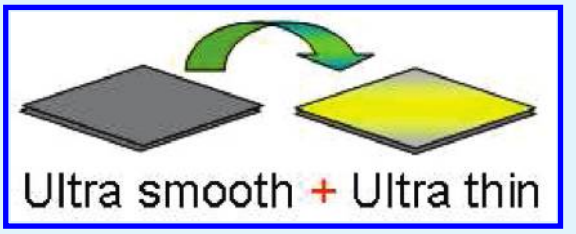

KEYWORDS: galvanic displacement, gold, ultrasmooth, thin films, X-ray photoelectron spectroscopy, self-limiting

1. INTRODUCTION

The integration of semiconductors and metals is considered an important step in a number of technologies, including integrated circuits,[1] sensing devices,[2] and more broadly, micro- and nanosystems technologies.[3] An efficient and attractive approach to integrate metals with semiconductors is metal deposition by galvanic displacement (GD). This process, a kind of electroless deposition, has gained interest mainly because of its versatility, ability to yield nanostructures with high purity, good substrate adhesion, and extremely high selectivity.[4] In GD reactions, metal ions in the plating bath are spontaneously reduced by the oxidation of the substrate itself, without external current sources or any reducing agents in the bath. The thermodynamic requirement for this process to occur is the appropriate values of the electrochemical potentials for both the deposited metal and the substrate that will be oxidized. Because of the simplicity of the GD process, especially considering the chemicals used, the setup and the final cost, this method provides an attractive alternative to sputtering or metal evaporation techniques.[5−8]

Many studies have focused on obtaining films, nanoparticles or nanostructures of different metals by GD on a variety of substrates, for diverse applications, including surface enhanced Raman spectroscopy (SERS),[9−16] catalyst deposition for chemical vapor growth of nanowires,[17−19] studies of protein interactions,[20] enhanced-performance photodiodes,[21] and electrochemical sensing.[22] One common feature in previous works is the fact that the substrate is usually dissolved in solution after being oxidized.[23−25] In the majority of cases, this dissolution is achieved by the addition of fluorinated species, such as HF or KF in the case of silicon, or by the inherent water solubility of the substrate oxide, as in the case of germanium.[26] By dissolving the substrate oxide, unreacted substrate atoms become available to supply electrons for the reduction and displacement of metal ions from solution so that the deposition of the metal film continues. The detailed mechanism of the process, especially during the early stages, remains an active topic of investigation. Recently, Sayed et al.[27] performed a thorough study of the initial steps in the Au GD process on Si(100) and Si(111) in the presence of fluoride, by high-resolution transmission electron microscopy combined with selected area electron diffraction and nanobeam diffraction. They concluded that the GD process, in aqueous conditions with fluorinated species, followed the Volmer−Weber growth mechanism in the early stages. With the aim of gaining a better understanding of gold deposition on silicon, we have investigated a new approach using a plating bath that does not contain any source of fluorinated species. In this way, the oxidized substrate is not removed during the process. Two previous studies have been reported on the deposition of silver and nickel on silicon without any fluorinated species, but in both cases the final morphology of the obtained metallic deposition were not discussed.[28,29] We have determined that the process is self-limited by the complete formation of an insulating oxide layer on the surface, which inhibits the transport of electrons from the substrate to the metal ions. In our experiments, we have achieved a maximum thickness of ~3.5 Å while conserving the smoothness of the original substrate. This thickness value is within the range of the expected thickness of an Au monolayer film.

Received: February 2, 2011
Accepted: April 8, 2011
Published: April 08, 2011

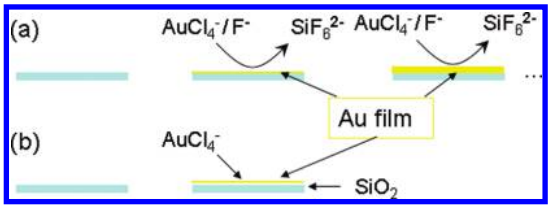

Figure 1. Galvanic displacement mechanism for (a) the conventional fluorinated process and (b) the presented fluoride-free method.

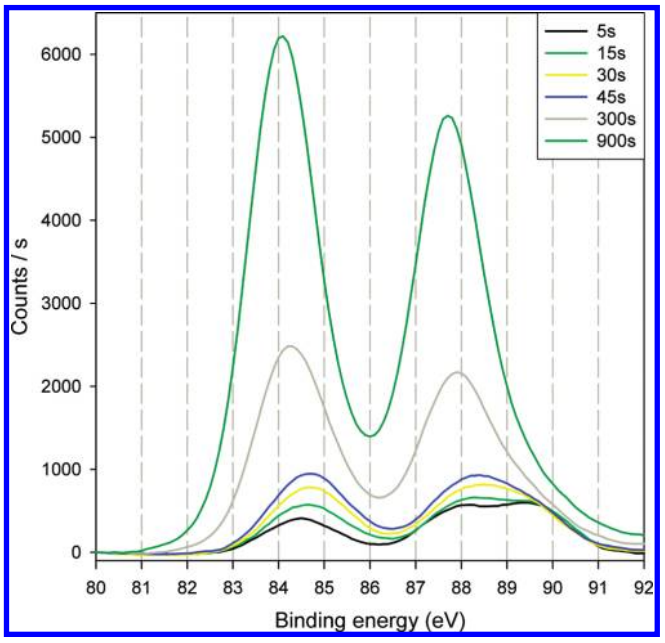

Figure 2. X-ray photoelectron spectra for the Au $4f_{7/2}$ region for the 0.02 mM $KAuCl_4$ dissolution at different immersion times.

2. EXPERIMENTAL SECTION

Sample Preparation. ⟨111⟩ Silicon 5 × 5 mm chips were degreased by sonication in acetone and isopropanol for 10 min and then rinsed with deionized water (18MΩ) before drying in gentle N_2. Ultraviolet ozone (UV−O) cleaning was applied for 10 min in order to remove organic materials from the surface. Native oxide layer was removed by immersing the chips in 48% concentrated HF for 1 min, triply rinsed in DI water and dried in N_2. Gold plating solution was prepared by dissolving the appropriate amount of $KAuCl_4$ in DI water to a final 2 mM concentration. 0.2 mM and 0.02 mM solutions were obtained by diluting the 2 mM solution in DI water. Silicon chips were immersed right after native oxide etching and left in solution for the desired time. Triple DI rinsing followed by N_2 drying was performed after incubation.

Characterization of Au Film. X-ray photoelectron spectroscopy (XPS) analysis was performed using Omicron analyzer (EA 125) using Al Kα to confirm metallic Au nature of the formed film as well as to quantify gold film thickness by Au to Si ratio signals. Au signal was integrated from 81 to 92 eV and Si signal was integrated from 97 to 106 eV to get the area signals of the two elements prior to calculating the ratio. In both cases, a background subtraction as well as a previous smoothing of the data were performed. Atomic force microscopy (AFM) operating in tapping mode (Digital Instruments multimode AFM Nanoscope IIIa) was used for film roughness measurements.

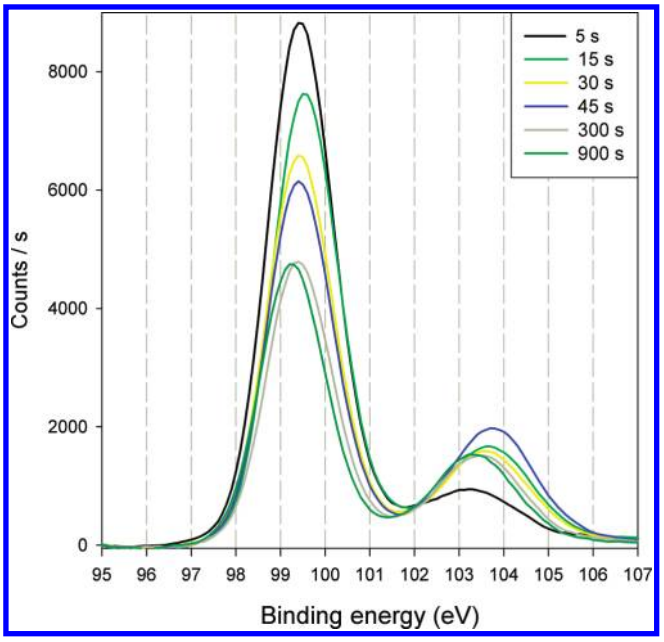

Figure 3. X-ray photoelectron spectra for the Si 2p region for the 0.02 mM $KAuCl_4$ dissolution at different immersion times.

3. RESULTS AND DISCUSSION

Ultrasmooth gold thin-film formation was achieved by a spontaneous galvanic displacement process, where the silicon substrate acts as the anode, being oxidized and providing electrons for the cathodic reaction, in this case the reduction of metal ions on the substrate surface. The novel aspect of the process presented here is that the dissolution of the silicon substrate is not carried out: in contrast to previously reported galvanic displacement processes on silicon (Figure 1a), where fluorine ions from HF or other fluoride salts react with the originally formed silicon oxide converting it into its soluble form of SiF_6^{2-}, in the present study no fluoride species is employed. Thus, the formation of silicon oxide on the substrate surface can act as a self-limiting step in the galvanic displacement process (Figure 1b).

Different concentrations of $KAuCl_4$ were tested in order to study the film formation rate dependence on this variable. For this purpose, 2, 0.2, and 0.02 mM $KAuCl_4$ dissolutions in deionized (DI) water were used as plating baths, with different immersion times, ranging from 5 to 900 s. Shorter times were avoided because of the difficulty in controlling the immersion and rinsing processes for less than 5 s. X-ray photoelectron spectroscopy was used to monitor the Au film thickness formation on the silicon substrates. Figures 2 and 3 show the Au 4f and the Si 2p regions for six different immersion times. In the Au 4f region and for short deposition times (from 5 to 45 s), the silicon satellite peak, expected at about 89 eV when using a nonmonochromatic X-ray source with an Al cathode, is clearly visible. The Si 2p region, shown in Figure 3, shows an increase in the silicon oxide peak at ∼103.5 eV as the immersion time increases. To null the effect of variations in signal intensity from run to run, it is more appropriate to examine the SiO_2 to Si (at 99.5 eV) peak intensity ratio. This ratio shows an increasing trend with time, which confirms the increase in SiO_2 formation and a decrease in the signal from Si underneath caused by the electron attenuation effects.

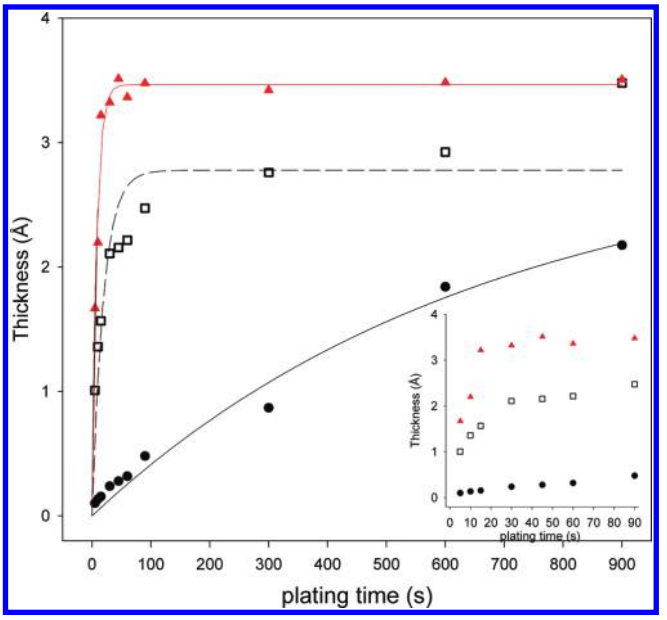

Figure 4. Nominal Au film thickness calculated from the Au to Si ratio for three different $KAuCl_4$ concentrations at different immersion times, and normalized to monolayer thickness. Black dots correspond to a 0.02 mM $KAuCl_4$ plating solution, hollow squares correspond to 0.2 mM plating solution and red triangles correspond to 2 mM plating solution. The curves are best fits to a simple kinetic model of irreversible monolayer adsorption, as discussed in the main text. The inset shows the first 90 s of deposition, for clarity.

Information about the Au film thickness can be obtained from the Au to Si signal peak intensity ratio. Following established analysis,[30] the Au film thickness, d_{Au}, is calculated taking into account the mean free path of electrons through the film, λ_{Au}, as well as the sensitivity factors, S, of these two elements shown in the following formula

$$d_{Au} = \lambda_{Au} \ln\left(1 + \frac{I_{Au}}{I_{Si}} \frac{S_{Si}}{S_{Au}}\right) \quad (1)$$

where the intensities I_{Au} and I_{Si} include the contributions of both components of the spin orbit doublets (7/2 and 5/2 for Au4f and 3/2 and 1/2 for Si2p), with the satellite Si peak intensity subtracted from the $Au4f_{5/2}$ region. Note that this formula is valid for homogeneous films, and therefore can be expected to be only qualitatively accurate for submonolayer coverage. In practice, as concerns our films, which are very smooth (vide infra), the formula is expected to be accurate once the derived thickness exceeds the nominal monolayer thickness, i.e., $d \geq 0.24$ nm.[31]

Figure 4 shows the nominal thickness of the Au film form eq.[1] as a function of immersion time for the three concentrations studied. With the proviso stated above, nominal thickness is a qualitative indicator of coverage. Thus, we also plot best fits to a simple kinetic model of irreversible monolayer adsorption, $d(t) = d_\infty(1 - \exp(-t/t_0))$. The fitted values of the asymptotic thickness d_∞ are 0.35, 0.28, and 0.30 nm in order of decreasing concentration, suggesting that the process is indeed self-limiting at a thickness of just above 1 ML.

The inset in the figure shows the data for short immersion times. As can be seen for the 2 mM concentration, a fast formation rate is achieved in the first 15 s. After that a much slower deposition rate is observed until a plateau is reached around 3.5 Å. For the 0.2 mM dissolution, the initial fast rise continues until 30 s, and after that the formation rate decreases. For this particular concentration a nearly perfect logarithmic trend is observed for the studied times, reaching the same thickness as the more concentrated dissolution after 900 s of immersion. Finally the 0.02 mM dissolution presents a linear trend until 90 s and after that a logarithmic trend is also observed. In this case, monolayer thickness is not yet reached even after 900 s of immersion. We can conclude that the films formed by this fluoride-less method using 0.2 mM or higher concentrations provides a simple and inexpensive way to obtain ultrathin Au films on silicon that are about one monolayer thin. The less concentrated (0.02 mM) solution needs higher immersion times to form a single layer according to the film thickness achieved for short immersion times.

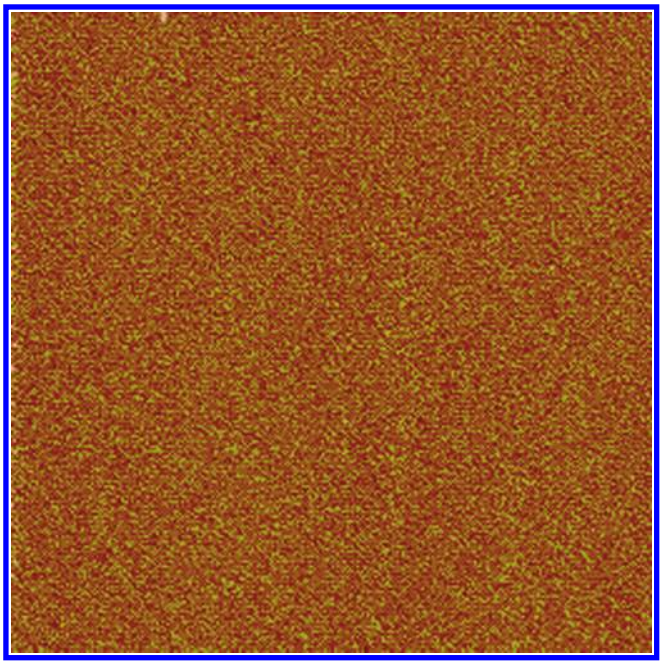

Figure 5. AFM image of the sample from 0.2 mM solution and after 60 s immersion time. Scanned area of 2 μm × 2 μm, z scale of 10 nm, and rms of ~0.72 nm.

Finally, to study the smoothness of the formed films, AFM studies were carried out on the deposited films. Figure 5 shows a representative plot for the film obtained from 0.2 mM solution and after 60 s immersion time. As can be observed no nanoparticles are formed, and in all cases the root-mean-square values obtained are below 1 nm, presenting the same roughness value as the starting Si substrate. Kelvin Prove Force Microscopy, performed simultaneously while doing the AFM scans revealed the uniformity in the surface potential, confirming the homogeneity of the formed metal film.

4. CONCLUSIONS

Atomically smooth gold films, with thickness of just one atomic monolayer, have been prepared on silicon by a simple galvanic displacement process. The key difference that allows the formation of ultrasmooth thin films is the lack of fluorinated species in the plating bath, which avoids the removal of the oxidized substrate, leading to a self-limiting process. The implications of this synthesis approach for catalyst deposition for

chemical vapor growth of semiconducting nanowires are currently under investigation. Other interesting implications that are open with the use of the presented substrates are VLS growth coupled with biofunctionalization and surface plasmon resonance studies or biosensing.

AUTHOR INFORMATION

Corresponding Author
*E-mail: maboudia@berkeley.edu. Telephone: +1 (510) 643-3489. Fax: +1 (510) 642-4778.

ACKNOWLEDGMENT

We acknowledge the support of the National Science Foundation, Grant EEC-0832819 (through the Center of Integrated Nanomechanical Systems) and DMR-0804646. Albert Gutés wishes to thank Comissionat per a Universitats i Recerca (CUR) del Departament d'Innovació, Universitat i Empresa de la Generalitat de Catalunya, for funding through the Beatriu de Pinós postdoctoral program. Dr. Ian Laboriante is also greafuly acknowledged for his help with the AFM measurements.

REFERENCES

(1) Cho, J. S. H.; Kang, H. K.; Wong, S. S.; Shacham-Diamand, Y. *MRS Bull.* **1993**, *18*, 31–38.
(2) Lin, K. W.; Chen, H. I.; Lu, C. T.; Tsai, Y. Y.; Chuang, H. M.; Chen, C. Y.; Liu, W. C. *Semicond. Sci. Technol.* **2003**, *18*, 615–619.
(3) Ieong, M.; Doris, B.; Kedzierski, J.; Rim, K.; Yang, M. *Science* **2004**, *306*, 2057–2060.
(4) Carraro, C.; Maboudian, R.; Magagnin, L. *Surf. Sci. Rep.* **2007**, *62*, 499–525.
(5) Piscopiello, E.; Tapfer, L.; Antisari, M. V.; Paiano, P.; Prete, P.; Lovergine, N. *Phys. Rev. B* **2008**, *78*, 035305.
(6) Piscopiello, E.; Tapfer, L.; Antisari, M. V.; Paiano, P.; Prete, P.; Lovergine, N. *Phys. Rev. B* **2009**, *80*, 049905.
(7) Sato, K.; Huang, W. J.; Bohra, F.; Sivaramakrishnan, S.; Tedjasaputra, A. P.; Zuo, J. M. *Phys. Rev. B* **2007**, *76*, 144113−1–144113−8.
(8) Arakaki, H.; Ohashi, K.; Sudou, T. *Semicond. Sci. Technol.* **2004**, *19*, 127–132.
(9) Bechelany, M.; Brodard, P.; Elias, J.; Brioude, A.; Michler, J.; Philippe, L. *Langmuir* **2010**, *26*, 14364–14371.
(10) Wang, Y.; Becker, M.; Wang, L.; Liu, J.; Scholz, R.; Peng, J.; Gösele, U.; Christiansen, S.; Kim, D. H.; Steinhart, M. *Nano Lett.* **2009**, *9*, 2384–2389.
(11) Gutes, A.; Carraro, C.; Maboudian, R. *ACS Appl. Mater. Interfaces* **2009**, *1*, 2551–2555.
(12) Brejna, P. R.; Griffiths, P. R.; Yang, J. *Appl. Spectrosc.* **2009**, *63*, 396–400.
(13) Brejna, P. R.; Griffiths, P. R. *Appl. Spectrosc.* **2010**, *64*, 493–499.
(14) Gutes, A.; Carraro, C.; Maboudian, R. *J. Am. Chem. Soc.* **2010**, *132*, 1476–1477.
(15) Sun, Y.; Wiederrecht, G. P. *Small* **2007**, *3*, 1964–1975.
(16) Zhao, H.; Fu, H.; Tian, C.; Ren, Z.; Tian, G. *Mater. Lett.* **2010**, *64*, 2255–2257.
(17) San Paulo, A.; Arellano, N.; Plaza, J. A.; He, R.; Carraro, C.; Maboudian, R.; Howe, R. T.; Bokor, J.; Yang, P. *Nano Lett.* **2007**, *7*, 1100–1104.
(18) Tseng, C.-H.; Tambe, M. J.; Lim, S. K.; Smith, M. J.; Gradecak, S. *Nanotechnology* **2010**, *21*, 165605.
(19) Cerruti, M.; Doerk, G.; Hernandez, G.; Carraro, C.; Maboudian, R. *Langmuir* **2009**, *26*, 432–437.
(20) Padmos, J. D.; Duchesne, P.; Dunbar, M.; Zhang, P. *J. Biomed. Mater. Res. Part A* **2010**, *95A*, 146–155.
(21) Blackwood, D. J.; Khoo, S. M. *Sol. Energy Mater. Sol. Cells* **2010**, *94*, 1201–1206.
(22) Gutes, A.; Laboriante, I.; Carraro, C.; Maboudian, R. *Sens. Actuator B, Chem.* **2010**, *147*, 681–686.
(23) Zhao, L.; Siu, A. C.-L.; Petrus, J. A.; He, Z.; Leung, K. T. *J. Am. Chem. Soc.* **2007**, *129*, 5730–5734.
(24) Ferralis, N.; Maboudian, R.; Carraro, C. *J. Phys. Chem. C* **2007**, *111*, 7508–7513.
(25) Magagnin, L.; Maboudian, R.; Carraro, C. *J. Phys. Chem B* **2002**, *106*, 401–407.
(26) Porter, L. A., Jr.; Choi, H. C.; Ribbe, A. E.; Buriak, J. M. *Nano Lett.* **2002**, *2*, 1067–1071.
(27) Sayed, S. Y.; Wang, F.; Malac, M.; Meldrum, A.; Egerton, R. F.; Buriak, J. M. *ACS Nano* **2009**, *3*, 2809–2817.
(28) Ye, W. C.; Tong, H.; Wang, C. M. *Microchim. Acta* **2005**, *152*, 85–88.
(29) Osaka, T.; Takano, N.; Komaba, S *Chem. Lett.* **1998**, No. 7, 657–658.
(30) Grant, J. T. *Surf. Interface Anal.* **1989**, *14*, 271–283.
(31) Citrin, P. H.; Wertheim, G. K.; Baer, Y. *Phys. Rev. Lett.* **1978**, *41*, 1425–1428.